On Media-based Modulation using RF Mirrors

Y. Naresh and A. Chockalingam
Department of Electrical Communication Engineering
Indian Institute of Science, Bangalore 560012, India
Email: ynr0109434@gmail.com, achockal@ece.iisc.ernet.in

***Abstract*—Media-based modulation (MBM) is a recently proposed modulation scheme which uses radio frequency (RF) mirrors at the transmit antenna(s) in order to create different channel fade realizations based on their ON/OFF status. These complex fade realizations constitute the modulation alphabet. MBM has the advantage of increased spectral efficiency and performance. In this paper, we investigate the performance of some physical layer techniques when applied to MBM. Particularly, we study the performance of i) MBM with generalized spatial modulation (GSM), ii) MBM with mirror activation pattern (MAP) selection based on an Euclidean distance (ED) based metric, and iii) MBM with feedback based phase compensation and constellation rotation. Our results show that, for the same spectral efficiency, GSM-MBM can achieve better performance compared to MIMO-MBM. Also, it is found that MBM with ED-based MAP selection results in improved bit error performance, and that phase compensation and MBM constellation rotation increases the ED between the MBM constellation points and improves the performance significantly.**

keywords: *Media-based modulation (MBM), RF mirrors, mirror activation pattern (MAP), MIMO-MBM, GSM-MBM, MAP selection, phase compensation, constellation rotation.*

I. Introduction

Traditionally, symbols chosen from complex modulation alphabets like quadrature amplitude modulation (QAM) and phase shift keying (PSK) are used to convey information bits, and complex fades introduced by the channel are viewed as detrimental effects that cause amplitude and phase distortion to the transmitted symbols. An alternate and interesting approach is to consider the complex channel fade coefficients themselves to constitute a modulation alphabet. One simple and known example of this approach is space shift keying (SSK) [1],[2], which can be briefly explained as follows.

1) SSK: Suppose there are two transmit antennas and one receive antenna. Assume rich scattering. Let $h_1 \sim \mathcal{CN}(0,1)$ and $h_2 \sim \mathcal{CN}(0,1)$ denote the complex channel fade coefficients from transmit antennas 1 and 2, respectively, to the receive antenna. Now, assuming that a tone of unit amplitude is transmitted by any one of the transmit antennas in a given channel use, $\mathbb{H} \triangleq \{h_1, h_2\}$ can be viewed as the underlying modulation alphabet, i.e., h_1 and h_2 are the *random* constellation points. The alphabet $\mathbb{H}$ therefore can convey $\log_2 |\mathbb{H}| = \log_2 2 = 1$ information bit. To realize this, if the information bit is 0, antenna 1 transmits the tone and antenna 2 remains silent, and if the information bit is 1, antenna 1 remains silent and antenna 2 transmits the tone. For this, it is enough to have only one transmit radio frequency (RF) chain, whose output is switched to either antenna 1 or antenna 2 depending on the information bit being 0 or 1, respectively. The modulation alphabet (i.e., $\mathbb{H}$) needs to be known at the receiver for detection, which can be obtained through pilot transmission and channel estimation. Note, however, that the transmitter need not know the alphabet $\mathbb{H}$. The information bit is detected using the estimated $\mathbb{H}$ at the receiver.

Similar to the binary SSK scheme with $|\mathbb{H}| = 2$ described above, higher-order SSK with $|\mathbb{H}| = n_t$ and $\mathbb{H} = \{h_1, h_2, \cdots, h_{n_t}\}$ can be realized using $n_t = 2^m$ transmit antennas, and sending the tone on an antenna chosen based on m information bits. Therefore, using $n_t = 2^m$ transmit antennas, SSK achieves a throughput of $m = \log_2 n_t$ bits per channel use (bpcu).

If the receiver has n_r receive antennas, then the alphabet $\mathbb{H}$ will consist of vector constellation points, i.e., $\mathbb{H} = \{\mathbf{h}_1, \mathbf{h}_2, \cdots, \mathbf{h}_{n_t}\}$, where $\mathbf{h}_j = [h_{1,j}\ h_{2,j}\ \cdots\ h_{n_r,j}]^T$, and $h_{i,j} \sim \mathcal{CN}(0,1)$ is the channel fade coefficient from jth transmit antenna to ith receive antenna (see Fig. 1(a)). Because of the increased dimensionality of the constellation points for increasing n_r, the performance of SSK improves significantly with increasing n_r. SSK has the advantages of i) requiring only one transmit RF chain and a $1 \times n_t$ RF switch for any n_t, and ii) yielding attractive performance at high bpcu values. A key drawback, however, is that SSK needs exponential increase in number of transmit antennas to increase the bpcu. For example, to achieve $m = 8$ bpcu, SSK requires $n_t = 2^8 = 256$ transmit antennas. This drawback of the need to have a large number of transmit antennas to increase the bpcu is significantly alleviated in the recently proposed media-based modulation (MBM) scheme [3]-[6], realized through the use of RF mirrors which are turned ON/OFF[1] on a channel use-by-channel use basis depending on information bits to 'modulate' the fade coefficients of the channel [6]. The basic MBM can be briefly explained as follows.

2) MBM: The basic version of MBM, like SSK, transmits a tone and uses the complex channel fade realizations themselves as the modulation alphabet [3]-[5]. While multiple transmit antennas are needed to create the complex fade symbols of the alphabet in SSK, MBM creates the complex fade symbols of the alphabet even with a single transmit antenna through the use of multiple RF mirrors [6]. This is achieved by placing a number of RF mirrors near the transmit antenna

[1]An RF mirror in ON status implies that the mirror allows the incident wave to pass through it transparently, and an OFF status implies that the mirror reflects back the incident wave.

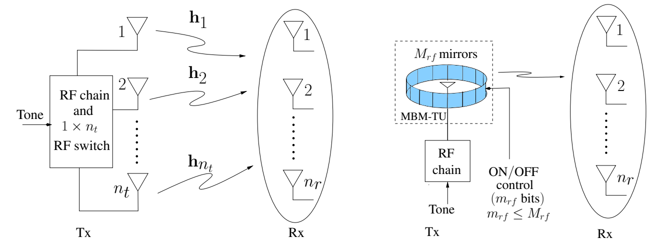

(a) SSK (b) MBM

Fig. 1. (a) SSK with constellation $\mathbb{H}_{\text{ssk}} = \{\mathbf{h}_1, \mathbf{h}_2, \cdots, \mathbf{h}_{n_t}\}$. (b) MBM with constellation $\mathbb{H}_{\text{mbm}} = \{\mathbf{h}_1, \mathbf{h}_2, \cdots, \mathbf{h}_{2^{m_{rf}}}\}$.

which transmits a tone. The ON/OFF status of these mirrors, which we call as the 'mirror activation pattern,' creates different fade realizations for different mirror activation patterns. This is typical in a rich scattering environment, since a small perturbation in the propagation environment will be augmented by reflections resulting in an independent channel, and the RF mirrors essentially create such perturbations that create independent fade realizations for different mirror activation patterns.

Consider a single transmit antenna. Let M_{rf} denote the total number of RF mirrors placed near the antenna. We call the unit comprising of a transmit antenna and the set of M_{rf} RF mirrors associated with it as the 'MBM transmit unit (MBM-TU)' (see Fig. 1(b)). Out of the M_{rf} available RF mirrors, let m_{rf}, where $1 \leq m_{rf} \leq M_{rf}$, denote the number of RF mirrors actually used. Each of these m_{rf} mirrors is turned ON or OFF in a given channel use based on one information bit. A realization of the ON/OFF status of all the m_{rf} mirrors, determined by m_{rf} information bits, is called a mirror activation pattern (MAP). Therefore, $2^{m_{rf}}$ MAPs are possible. Each of these patterns results in a different realization of the channel fade, resulting in an MBM alphabet of size $|\mathbb{H}| = 2^{m_{rf}}$. Therefore, *MBM can convey m_{rf} information bits in one channel use, where m_{rf} is the number of RF mirrors used. That is, the bpcu in MBM scales linearly with the number of RF mirrors used. This is one of the key advantages of MBM over SSK, because the bpcu in SSK scales only logarithmically in the number of transmit antennas, given by $\log_2 n_t$.*

As in SSK, in MBM also the alphabet $\mathbb{H}$ needs to be known at the receiver and not at the transmitter. All the $|\mathbb{H}| = 2^{m_{rf}}$ complex fade symbols in the MBM alphabet need to be estimated through pilot transmission. This implies that *the number of channel uses needed for pilot transmission in MBM grows exponentially with the number of RF mirrors used. Channel sounding to learn the alphabet a priori, therefore, is a key issue in MBM.*

MBM has been shown to achieve significant performance gains compared to conventional modulation schemes [3]-[5]. Even with a single transmit antenna and n_r receive antennas, MBM has been shown to achieve significant energy savings compared to a conventional $n_r \times n_t$ MIMO system with $n_r = n_t$ [3]. It has also been shown that MBM with 1 transmit and n_r receive antennas over a static multipath channel asymptotically achieves the capacity of n_r parallel AWGN channels [4]. Implementation of an MBM-TU consisting of $M_{rf} = 14$ RF mirrors placed in a compact cylindrical structure with a dipole transmit antenna element placed at the center of the cylindrical structure has been reported in [6].

3) SM, GSM, MIMO: The need to exponentially increase the number of transmit antennas to increase the bpcu in SSK can be alleviated by allowing the transmission of M-ary QAM/PSK symbols on the chosen antenna instead of a tone. This allows an additional $\log_2 M$ bits to be conveyed per channel use by the QAM/PSK symbol. This scheme is called the spatial modulation (SM) scheme, which achieves a spectral efficiency of $\log_2 n_t + \log_2 M$ bpcu [7],[8],[9]. A further generalization is to use more than one transmit RF chain (say, n_{rf} transmit RF chains, $1 \leq n_{rf} \leq n_t$), and transmit n_{rf} QAM/PSK symbols through these RF chains. This scheme is called as the generalized spatial modulation (GSM) scheme, whose spectral efficiency is given by $\lfloor \log_2 \binom{n_t}{n_{rf}} \rfloor + n_{rf} \log_2 M$ bpcu [10],[11],[12]. For $n_{rf} = n_t$, the GSM scheme specializes to the well known MIMO (spatial multiplexing) scheme, whose spectral efficiency is given by $n_t \log_2 M$ bpcu.

4) SM-MBM, GSM-MBM, MIMO-MBM: Multiple MBM-TUs (i.e., multiple transmit antennas, each having its own set of RF mirrors) can be used to increase the spectral efficiency in MBM. Also, like QAM/PSK symbols (as in SM) and additional transmit RF chains (as in GSM, MIMO) could be used to increase the bpcu beyond that can be achieved using SSK, one could use a similar approach to increase the bpcu beyond that can be achieved using the basic MBM. Spatial modulation when used with MBM is referred to as the SM-MBM scheme, whose spectral efficiency is given by $m_{rf} + \lfloor \log_2 n_{tu} \rfloor + \log_2 M$ bpcu, where n_{tu} is the number of MBM-TUs. Similarly, GSM and MIMO (spatial multiplexing) when used with MBM are called GSM-MBM and MIMO-MBM, respectively. The spectral efficiency of GSM-MBM is given by $n_{rf} m_{rf} + \lfloor \log_2 \binom{n_{tu}}{n_{rf}} \rfloor + n_{rf} \log_2 M$ bpcu. The spectral efficiency of MIMO-MBM is given by $n_{tu} m_{rf} + n_{tu} \log_2 M$ bpcu. The performance of MIMO-MBM has been studied in [6], where it has been shown that MIMO-MBM can achieve better performance compared to conventional MIMO. GSM-MBM performance has not been studied in [6]. One of our contributions in this paper is to present the performance of GSM-MBM and compare it with that of MIMO-MBM.

5) MBM viewed as an instance of index modulation: MBM can be viewed as an instance of index modulation, where information bits are conveyed through the indices of certain transmit entities that get involved in the transmission. Indexing transmit antennas in multi-antenna systems (e.g., SSK, SM, GSM [1],[2],[7]-[12]), indexing subcarriers in multi-carrier systems [13]-[16], indexing both transmit antennas and subcarriers [17], and indexing precoders [18] are examples of such instances. In this context, MBM also can be viewed as an index modulation scheme, where RF mirrors act as the transmit entities that are indexed to convey information bits. In SM-MBM and GSM-MBM, indexing is done both on the MBM-TUs as well as the RF mirrors in each of the chosen

MBM-TUs for transmission.

A common observation in index modulation schemes is that, to achieve a certain bpcu, because of the indexing bits, the number of bits conveyed through QAM/PSK symbols can be reduced compared to that in conventional modulation schemes. That is, to achieve a certain bpcu, index modulation schemes can use a smaller-sized QAM/PSK alphabet compared that in conventional modulation schemes. This results in an signal-to-noise (SNR) advantage in favor of index modulation. Through the indexing of RF mirrors, MBM also can achieve such SNR gains over conventional modulation schemes.

6) Contributions in this paper: In this paper, we investigate the performance of some physical layer techniques when applied to MBM. These techniques include generalized spatial modulation, MAP selection (analogous to antenna selection in MIMO systems), and phase compensation and constellation rotation. Our contributions in this paper can be summarized as follows.

- We study the performance of MBM with generalized spatial modulation (referred to as GSM-MBM), and compare its performance with that MIMO-MBM. Our results show that, for the same spectral efficiency, GSM-MBM can achieve better performance compared to MIMO-MBM. An union bound based upper bound on the average bit error probability (BEP) of GSM-MBM is shown to be tight for moderate-to-high SNRs.
- We investigate a MAP selection scheme based on an Euclidean distance (ED) based metric, and compare its bit error performance with that of a mutual information (MI) based MAP selection scheme. The ED-based MAP selection scheme is found to perform better than the MI-based MAP selection scheme by several dBs. The diversity order achieved by the ED-based MAP selection scheme is shown to be $n_r(2^{M_{rf}} - 2^{m_{rf}} + 1)$, which is validated through simulations as well.
- We investigate a scheme with feedback based phase compensation and MBM constellation rotation, which increases the ED between the constellation points and improves the bit error performance significantly.

The rest of this paper is organized as follows. Section II presents the GSM-MBM scheme and its performance. Section III presents the ED-based MAP selection scheme and its performance. Section IV presents the feedback based phase compensation and constellation rotation scheme and its performance. Conclusions are presented in V.

II. GSM-MBM scheme

In this section, we introduce the GSM-MBM scheme and analyze its bit error performance. The GSM-MBM transmitter is shown in Fig. 2. It consists of n_{tu} MBM-TUs, n_{rf} transmit RF chains, $1 \leq n_{rf} \leq n_{tu}$, and an $n_{rf} \times n_{tu}$ RF switch. In each MBM-TU, m_{rf} RF mirrors are used. In GSM-MBM, information bits are conveyed using MBM-TU indexing, RF mirror indexing, and QAM/PSK symbols, as follows. In each channel use, $i)$ n_{rf} out of n_{tu} MBM-TUs are selected using $\lfloor \log_2 \binom{n_{tu}}{n_{rf}} \rfloor$ bits, $ii)$ on the selected n_{rf} MBM-TUs, n_{rf} M-ary QAM/PSK symbols (formed using $n_{rf} \log_2 M$ bits) are transmitted, and $iii)$ the ON/OFF status of the m_{rf} mirrors in each of the selected MBM-TU is controlled by m_{rf} bits (so that all the $n_{rf}m_{rf}$ mirrors in the selected n_{rf} MBM-TUs are controlled by $n_{rf}m_{rf}$ bits). Therefore, the achieved rate in bpcu is given by

$$\eta = \underbrace{\left\lfloor \log_2 \binom{n_{tu}}{n_{rf}} \right\rfloor}_{\text{MBM-TU index bits}} + \underbrace{n_{rf}m_{rf}}_{\text{mirror index bits}} + \underbrace{n_{rf}\log_2 M}_{\text{QAM/PSK symbol bits}} \ \text{bpcu}. \quad (1)$$

GSM-MBM specializes to SIMO-MBM when $n_{tu} = n_{rf} = 1$, to SM-MBM when $n_{tu} > 1$ and $n_{rf} = 1$, and to MIMO-MBM when $n_{tu} > 1$ and $n_{rf} = n_{tu}$.

A. GSM signal set

Let $\mathbb{A}$ denote the M-ary QAM/PSK alphabet used. In a given channel use, each of the n_{tu} MBM-TUs is made ON (and a symbol from $\mathbb{A}$ is sent) or OFF (which is equivalent to sending 0) based on information bits. Let us call a realization of the ON/OFF status of the n_{tu} MBM-TUs as a 'MBM-TU activation pattern'. A total of $\binom{n_{tu}}{n_{rf}}$ MBM-TU activation patterns are possible. Out of them, only $2^{\lfloor \log_2 \binom{n_{tu}}{n_{rf}} \rfloor}$ are needed for signaling. Let $\mathbb{S}_t$ denote the set of these $2^{\lfloor \log_2 \binom{n_{tu}}{n_{rf}} \rfloor}$ MBM-TU activation patterns chosen from the set all possible MBM-TU activation patterns. A mapping is done between combinations of $\lfloor \log_2 \binom{n_{tu}}{n_{rf}} \rfloor$ bits to MBM-TU activation patterns in $\mathbb{S}_t$. The GSM signal set, denoted by $\mathbb{S}_{\text{gsm}}$, is the set of $n_{tu} \times 1$-sized GSM signal vectors that can be transmitted, which is given by

$$\mathbb{S}_{\text{gsm}} = \big\{ \mathbf{s} : s_j \in \mathbb{A} \cup \{0\}, \ \|\mathbf{s}\|_0 = n_{rf}, \ \mathcal{I}(\mathbf{s}) \in \mathbb{S}_t \big\}, \quad (2)$$

where $\mathbf{s}$ is the $n_{tu} \times 1$ transmit vector, s_j is the jth entry of $\mathbf{s}$, $j = 1, 2, \cdots, n_{tu}$, $\|\mathbf{s}\|_0$ is the l_0-norm of the vector $\mathbf{s}$, and $\mathcal{I}(\mathbf{s})$ is a function that gives the MBM-TU activation pattern for $\mathbf{s}$. For example, when $\mathbb{A}$ is BPSK, $n_{tu} = 4$ and $n_{rf} = 3$, $\mathbf{s} = [+1 \ \ 0 \ -1 \ -1]^T$ is a valid GSM signal vector, and $\mathcal{I}(\mathbf{s})$ in this case is given by $\mathcal{I}(\mathbf{s} = [+1 \ \ 0 \ -1 \ -1]^T) = [1 \ 0 \ 1 \ 1]^T$.

B. GSM-MBM received signal

In GSM-MBM, in addition to the bits conveyed by the GSM signal vector, the channel fade symbols created by the RF mirrors in the active MBM-TUs also convey additional bits. Let n_r denote the number of receive antennas. Since m_{rf} mirrors are used in each MBM-TU, the number of mirror activation patterns (MAPs) on each MBM-TU is given by $N_m = 2^{m_{rf}}$. Let $\mathbb{S}_m$ denote the set of all N_m MAPs per MBM-TU. Let $\mathbb{H}^j$ denote the MBM alphabet of size N_m, consisting of $n_r \times 1$-sized vector constellation points formed using the channel fade coefficients corresponding to the N_m MAPs of jth MBM-TU to the receive antennas. Let $\mathbf{h}_k^j = [h_{1,k}^j \ h_{2,k}^j \ \cdots \ h_{n_r,k}^j]^T$ denote the $n_r \times 1$-sized channel coefficient vector at the receiver for the kth MAP of the jth MBM-TU, where $h_{i,k}^j \sim \mathcal{CN}(0,1)$ is the fade coefficient corresponding to the kth MAP of jth MBM-TU to the ith receive antenna, $i = 1, 2, \cdots, n_r$,

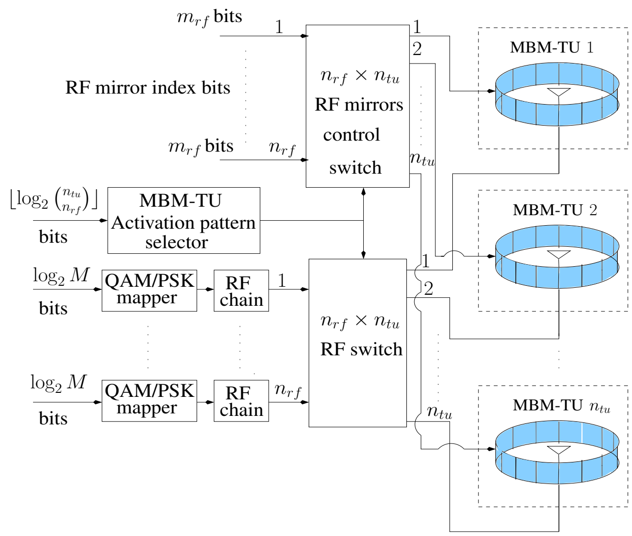

Fig. 2. GSM-MBM transmitter.

$j = 1, 2, \cdots, n_{tu}$, and $k = 1, 2, \cdots, N_m$. We then have $\mathbb{H}^j = \{\mathbf{h}_1^j, \mathbf{h}_2^j, \cdots, \mathbf{h}_{N_m}^j\}$. Let $s_j \in \mathbb{A}$ denote the M-ary QAM/PSK symbol transmitted on the jth MBM-TU. The received signal vector $\mathbf{y} = [y_1\ y_2\ \cdots\ y_{n_r}]^T$ in a given channel use is then given by

$$\mathbf{y} = \sum_{j=1}^{n_{tu}} s_j \mathbf{h}_{l_j}^j + \mathbf{n}, \tag{3}$$

where $s_j \in \mathbb{A} \cup \{0\}$, $l_j \in \{1, \cdots, N_m\}$ is the index of the MAP chosen on the jth MBM-TU, $\mathbf{h}_{l_j}^j \in \mathbb{H}^j$, and $\mathbf{n} = [n_1\ n_2\ \cdots\ n_{n_r}]^T$ is the additive noise vector, whose elements are i.i.d. and distributed as $\mathcal{CN}(0, \sigma^2)$. Let $\mathbf{H}^j = [\mathbf{h}_1^j\ \mathbf{h}_2^j\ \cdots\ \mathbf{h}_{N_m}^j]$ denote the $n_r \times N_m$ channel matrix corresponding to the jth MBM-TU. The received vector $\mathbf{y}$ in (3) can be written as

$$\mathbf{y} = \sum_{j=1}^{n_{tu}} s_j \mathbf{H}^j \mathbf{e}_{l_j} + \mathbf{n}, \tag{4}$$

where $\mathbf{e}_{l_j}$ is an $N_m \times 1$ vector whose l_jth coordinate is 1 and all other coordinates are zeros. Now, defining $\mathbf{H} = [\mathbf{H}^1\ \mathbf{H}^2\ \cdots\ \mathbf{H}^{n_{tu}}]$ as the overall $n_r \times N_m n_{tu}$ channel matrix, we can write $\mathbf{y}$ as

$$\mathbf{y} = \mathbf{H}\mathbf{x} + \mathbf{n}, \tag{5}$$

where $\mathbf{x}$ belongs to the GSM-MBM signal set $\mathbb{S}_{\text{gsm-mbm}}$, which is given by

$$\mathbb{S}_{\text{gsm-bmb}} = \Big\{\mathbf{x} = [\mathbf{x}_1^T\ \mathbf{x}_2^T\ \cdots\ \mathbf{x}_{n_{tu}}^T]^T : \mathbf{x}_j = s_j \mathbf{e}_{l_j}, \\ l_j \in \{1, \cdots, N_m\};\ \ \mathbf{s} = [s_1\ s_2\ \cdots\ s_{n_{tu}}]^T \in \mathbb{S}_{\text{gsm}}\Big\}. \tag{6}$$

The maximum likelihood (ML) decision rule is given by

$$\hat{\mathbf{x}} = \underset{\mathbf{x} \in \mathbb{S}_{\text{gsm-mbm}}}{\text{argmin}} \ \|\mathbf{y} - \mathbf{H}\mathbf{x}\|^2. \tag{7}$$

The bits corresponding to $\hat{\mathbf{x}}$ are demapped as follows: i) the MBM-TU activation pattern for $\mathbf{s}$ gives $\lfloor \log_2 \binom{n_{tu}}{n_{rf}} \rfloor$ MBM-TU index bits, ii) the non-zero entries in $\mathbf{s}$ gives $n_{rf} \log_2 M$ QAM/PSK bits, and iii) for each non-zero location j in $\mathbf{s}$, l_j gives m_{rf} mirror index bits; since $\mathbf{s}$ has n_{rf} non-zero entries, a total of $n_{rf} m_{rf}$ mirror index bits are obtained from l_j's.

C. Average BEP analysis

The ML decision rule for GSM-MBM is given by (7). The conditional pairwise error probability (PEP) of $\mathbf{x}$ being decoded as $\tilde{\mathbf{x}}$ can be written as

$$P(\mathbf{x} \to \tilde{\mathbf{x}} | \mathbf{H}) = P\left(\|\mathbf{y} - \mathbf{H}\mathbf{x}\|^2 > \|\mathbf{y} - \mathbf{H}\tilde{\mathbf{x}}\|^2 | \mathbf{H}\right). \tag{8}$$

From (5), we can write (8) as

$$\begin{aligned} P(\mathbf{x} \to \tilde{\mathbf{x}} | \mathbf{H}) &= P\left(\|\mathbf{n}\|^2 > \|\mathbf{H}(\mathbf{x} - \tilde{\mathbf{x}}) + \mathbf{n}\|^2 | \mathbf{H}\right) \\ &= P\left(2\Re\left(\mathbf{n}^\dagger \mathbf{H}(\tilde{\mathbf{x}} - \mathbf{x})\right) > \|\mathbf{H}(\mathbf{x} - \tilde{\mathbf{x}})\|^2 | \mathbf{H}\right), \end{aligned} \tag{9}$$

where $\Re(.)$ denotes real part, $(.)^\dagger$ denotes conjugate transpose, and $2\Re\left(\mathbf{n}^\dagger \mathbf{H}(\tilde{\mathbf{x}} - \mathbf{x})\right)$ is a Gaussian random variable with zero mean and variance $2\sigma^2 \|\mathbf{H}(\mathbf{x} - \tilde{\mathbf{x}})\|^2$. Therefore,

$$P(\mathbf{x} \to \tilde{\mathbf{x}} | \mathbf{H}) \ = \ Q\left(\sqrt{\|\mathbf{H}(\mathbf{x} - \tilde{\mathbf{x}})\|^2 / 2\sigma^2}\right). \tag{10}$$

The computation of the unconditional PEP $P(\mathbf{x} \to \tilde{\mathbf{x}})$ requires the expectation of the $Q(.)$ function in (10) w.r.t. $\mathbf{H}$, which can be obtained as follows [19]:

$$\begin{aligned} P(\mathbf{x} \to \tilde{\mathbf{x}}) &= \mathbb{E}_{\mathbf{H}}\{P(\mathbf{x} \to \tilde{\mathbf{x}} | \mathbf{H})\} \\ &= \mathbb{E}_{\mathbf{H}}\left\{Q\left(\sqrt{\|\mathbf{H}(\mathbf{x} - \tilde{\mathbf{x}})\|^2 / 2\sigma^2}\right)\right\} \\ &= f(\beta)^{n_r} \sum_{i=0}^{n_r - 1} \binom{n_r - 1 + i}{i} (1 - f(\beta))^i, \end{aligned} \tag{11}$$

where $f(\beta) \triangleq \frac{1}{2}\left(1 - \sqrt{\frac{\beta}{1+\beta}}\right)$, and $\beta \triangleq \frac{\|\mathbf{x} - \tilde{\mathbf{x}}\|^2}{4\sigma^2}$. Now, an upper bound on the average BEP for GSM-MBM based on union bounding can be obtained as

$$P_B \leq \frac{1}{2^\eta} \sum_{\mathbf{x}} \sum_{\tilde{\mathbf{x}} \neq \mathbf{x}} P(\mathbf{x} \to \tilde{\mathbf{x}}) \frac{\delta(\mathbf{x}, \tilde{\mathbf{x}})}{\eta}, \tag{12}$$

where $\delta(\mathbf{x}, \tilde{\mathbf{x}})$ is the number of bits in which $\mathbf{x}$ differs from $\tilde{\mathbf{x}}$. The BEP upper bound for SIMO-MBM can be obtained from the above expression by setting $n_{tu} = n_{rf} = 1$. Likewise, the BEP upper bound for MIMO-MBM can be obtained by setting $n_{tu} > 1$ and $n_{rf} = n_{tu}$.

D. Results and discussions

1) Comparison between systems with and without RF mirrors: First, in Fig. 3, we illustrate the effectiveness of SIMO-MBM scheme with RF mirrors compared to other popularly known multi-antenna schemes without RF mirrors. The bpcu is fixed at 8 bpcu for all the schemes considered. All the schemes use $n_r = 16$ and ML detection. The schemes considered are:

1) SIMO-MBM with $n_{tu} = n_{rf} = 1$, $m_{rf} = 6$, and 4 QAM (6 bits from indexing RF mirrors and 2 bits from one 4-QAM symbol).
2) MIMO (spatial multiplexing) with $n_t = 2$, $n_{rf} = 2$, and 16-QAM (8 bits from two 16-QAM symbols).
3) MIMO (spatial multiplexing) with $n_t = 4$, $n_{rf} = 4$, and 4-QAM (8 bits from four 4-QAM symbols).

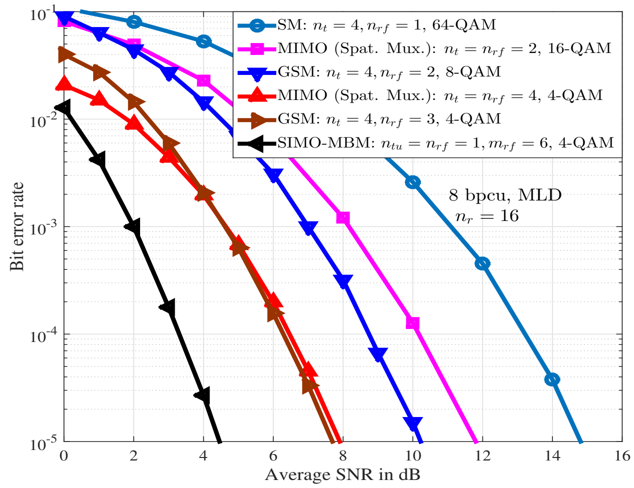

Fig. 3. BER performance comparison between SIMO-MBM with RF mirrors and other multi-antenna schemes without RF mirrors (MIMO, SM, GSM) at 8 bpcu and $n_r = 16$.

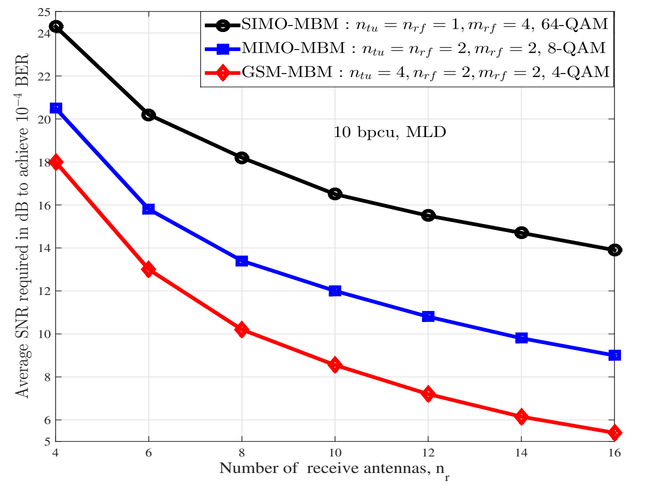

Fig. 5. Average SNR required to achieve 10^{-4} BER as a function of n_r for the three schemes considered in Fig. 4 (SIMO-MBM, MIMO-MBM, GSM-MBM) at 10 bpcu.

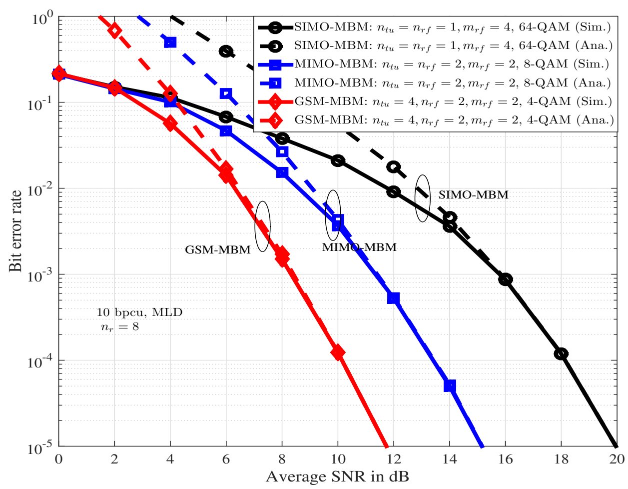

Fig. 4. BER performance of SIMO-MBM, MIMO-MBM, and GSM-MBM with $n_r = 8$, and 10 bpcu. SIMO-MBM: $n_{tu} = n_{rf} = 1$, $m_{rf} = 4$, 64-QAM. MIMO-MBM: $n_{tu} = n_{rf} = 2$, $m_{rf} = 2$, 8-QAM. GSM-MBM: $n_{tu} = 4$, $n_{rf} = 2$, $m_{rf} = 2$, 4-QAM.

4) SM with $n_t = 4$, $n_{rf} = 1$, and 64-QAM (2 bits from indexing antennas and 6 bits from one 64-QAM symbol).
5) GSM with $n_t = 4$, $n_{rf} = 2$, and 8-QAM (2 bits from indexing antennas and 6 bits from two 8-QAM symbols).
6) GSM with $n_t = 4$, $n_{rf} = 3$, and 4-QAM (2 bits from indexing antennas and 6 bits from three 4-QAM symbols).

It can be seen that SIMO-MBM scheme with RF mirrors achieves significantly better bit error rate (BER) performance compared to other multi-antenna schemes which do not use RF mirrors. This illustrates the BER performance advantage possible with systems that employ media-based modulation using RF mirrors.

2) Comparison between SIMO-MBM, MIMO-MBM, GSM-MBM: Next, we evaluate the BER performance of GSM-MBM scheme through analysis and simulations. We also evaluate the bit error performance of SIMO-MBM and MIMO-MBM schemes for comparison. We compare these three schemes for the same bpcu. Figure 4 shows the BER performance comparison between the following schemes, namely SIMO-MBM, MIMO-MBM, and GSM-MBM schemes, all achieving the same 10 bpcu:

1) SIMO-MBM using $n_{tu} = n_{rf} = 1$, $m_{rf} = 4$, and 64-QAM (4 bits from indexing mirrors and 6 bits from one 64-QAM symbol).
2) MIMO-MBM using $n_{tu} = n_{rf} = 2$, $m_{rf} = 2$, and 8-QAM (4 bits from indexing mirrors, 6 bits from two 8-QAM symbols).
3) GSM-MBM using $n_{tu} = 4$, $n_{rf} = 2$, $m_{rf} = 2$, and 4-QAM (4 bits from indexing mirrors, 2 bits from indexing MBM-TUs, and 4 bits from two 4-QAM symbols).

All the three schemes use $n_r = 8$ and ML detection. The following observations can be made from Fig. 4. The analytical upper bound is tight for moderate-to-high SNRs. MIMO-MBM achieves better performance compared to SIMO-MBM. For example, at a BER of 10^{-4}, MIMO-MBM requires about 4.4 dB less SNR compared to SIMO-MBM. Also, GSM-MBM is found to perform better than both SIMO-MBM and MIMO-MBM. For example, at 10^{-4} BER, GSM-MBM gives an SNR advantage of about 3.2 dB and 7.8 dB over MIMO-MBM and SIMO-MBM, respectively. This is because more bits are conveyed through spatial indexing in GSM-MBM (i.e., through indexing of mirrors and MBM-TUs), which results in a reduced QAM size (4-QAM for GSM-MBM compared to 8-QAM and 64-QAM for MIMO-MBM and SIMO-MBM, respectively).

Figure 5 shows a performance comparison between SIMO-MBM, MIMO-MBM, and GSM-MBM schemes with 10 bpcu as a function of n_r. It shows the average SNR required to achieve a target BER of 10^{-4} for increasing values of n_r in the three schemes considered in Fig. 4. It can be seen that, as observed in Fig. 4, GSM-MBM achieves significant SNR gains compared to MIMO-MBM and SIMO-MBM. The results, therefore, show that GSM is an attractive physical layer technique which can be beneficial when used in MBM. Note that SIMO-MBM, MIMO-MBM, and GSM-MBM schemes do not need any feedback for their operation. In the next two sections, we study how feedback based physical layer techniques can be beneficial when used in MBM schemes.

III. ED-BASED MAP SELECTION

In practice, an MBM-TU may be designed to have more RF mirrors available for use than the number of RF mirrors actually used. Let M_{rf} denote the number of mirrors available in an MBM-TU[1]. This means that the maximum number of channel fade symbols (aka MBM constellation points) that can be generated by the MBM-TU is $2^{M_{rf}}$, i.e., one MBM constellation point per MAP. But not all $2^{M_{rf}}$ MAPs, and hence not all the corresponding MBM constellation points may be used. Only a subset of the $2^{M_{rf}}$ MAPs, say $2^{m_{rf}}$, $m_{rf} \leq M_{rf}$, MAPs are actually used to convey m_{rf} bits through indexing mirrors. Now, one can choose the best subset of $2^{m_{rf}}$ MAPs from the set of all $2^{M_{rf}}$ possible MAPs. In other words, select the best $2^{m_{rf}}$ among the $2^{M_{rf}}$ MBM constellation points and form the MBM alphabet $\mathbb{H}$ of size $|\mathbb{H}| = 2^{m_{rf}}$ constellation points. Such MAP selection in MBM can be viewed as analogous to transmit antenna selection (TAS) in multi-antenna systems, where a subset of antennas among the available antennas is selected for transmission and the selection is based on channel knowledge.

Here, we consider MAP selection in MIMO-MBM. Let $\mathbb{S}_{\text{all}}$ denote the set of all possible MAPs per MBM-TU. So, $|\mathbb{S}_{\text{all}}| = 2^{M_{rf}}$. Let $\mathbb{S}_{\text{sub}}$ denote a possible subset of $\mathbb{S}_{\text{all}}$, where $|\mathbb{S}_{\text{sub}}| = 2^{m_{rf}}$, $m_{rf} \leq M_{rf}$. The receiver estimates all the $|\mathbb{S}_{\text{all}}|$ MBM constellation points for every coherence interval, selects the best $|\mathbb{S}_{\text{sub}}|$ constellation points among them, and conveys the indices of the corresponding MAPs to the transmitter. The transmitter uses these selected MAPs to index the mirrors in that coherence interval.

We consider two MAP selection schemes, one that uses an MI based metric (which is studied in [4],[5]) and another that uses an ED based metric. The ED based antenna selection has been studied in the context of SM systems in [20]. In what follows in this section, we present these MAP selection schemes and their BER performance.

A. MI-based MAP selection

In [4],[5], a selection scheme that chooses the MBM constellation points with the highest energies is studied. This scheme is motivated by the observation that mutual information is proportional to the energy (norm) of the MBM constellation point, and hence selecting the MBM constellation points with the highest energies maximizes the mutual information.

[1]A typical implementation of an MBM-TU reported in the literature has $M_{rf} = 14$ RF mirrors available [6].

Let $\{l_{j1}, l_{j2}, \cdots, l_{j|\mathbb{S}_{\text{sub}}|}\}$ be the set of MAP indices corresponding to the $|\mathbb{S}_{\text{sub}}|$ largest energies for the jth MBM-TU, which expects that

$$\|\mathbf{h}^j_{l_{j1}}\|^2 \geq \|\mathbf{h}^j_{l_{j2}}\|^2 \geq \cdots \geq \|\mathbf{h}^j_{l_{j|\mathbb{S}_{\text{sub}}|}}\|^2 \geq \cdots \geq \|\mathbf{h}^j_{l_{j|\mathbb{S}_{\text{all}}|}}\|^2,$$

$j = 1, 2, \cdots, n_{t_u}$. The received signal vector considering this MAP selection is given by

$$\mathbf{y} = \mathbf{H}_{\text{MI}}\mathbf{x} + \mathbf{n}, \tag{13}$$

where $\mathbf{H}_{\text{MI}}$ is the channel matrix of size $n_r \times n_{tu}|\mathbb{S}_{\text{sub}}|$, given by $\mathbf{H}_{\text{MI}} = [\mathbf{H}^1_{\text{MI}}\ \mathbf{H}^2_{\text{MI}}\ \cdots\ \mathbf{H}^{n_{tu}}_{\text{MI}}]$, and $\mathbf{H}^j_{\text{MI}} = [\mathbf{h}^j_{l_{j1}}\ \mathbf{h}^j_{l_{j2}}\ \cdots\ \mathbf{h}^j_{l_{j|\mathbb{S}_{\text{sub}}|}}]$. That is, the selected MBM vector constellation points of all the MBM-TUs form the column vectors of the $\mathbf{H}_{\text{MI}}$ matrix. At the receiver, ML detection is performed using the knowledge of the channel matrix $\mathbf{H}_{\text{MI}}$. It can be seen that the order of complexity of this MAP selection scheme per MBM-TU is $\mathcal{O}\left(|\mathbb{S}_{\text{all}}|\right)$. Hence, the order of total complexity is $\mathcal{O}\left(n_{tu}|\mathbb{S}_{\text{all}}|\right)$.

B. ED-based MAP selection

Another way to do MAP selection is to choose the best MBM constellation points based on ED. Let $\mathcal{I}^j$ denote the collection of sets of MAP indices corresponding to the enumerations of the $\binom{|\mathbb{S}_{\text{all}}|}{|\mathbb{S}_{\text{sub}}|}$ combinations of selecting $|\mathbb{S}_{\text{sub}}|$ out of $|\mathbb{S}_{\text{all}}|$ MAPs of the jth MBM-TU. Let $\mathcal{L}$ denote the following set, defined as

$$\mathcal{L} = \left\{\mathbb{L} = \{\mathbb{L}^1, \mathbb{L}^2, \cdots, \mathbb{L}^{n_{tu}}\} : \mathbb{L}^j \in \mathcal{I}^j, j = \{1, \cdots, n_{tu}\right\}.$$

Among the $|\mathcal{L}|$ possible sets, choose that set which maximizes the minimum Euclidean distance among all possible transmit vectors. That is,

$$\mathbb{L}_{\text{ED}} = \underset{\mathbb{L}\in\mathcal{L}}{\text{argmax}} \left\{ \min_{\substack{\mathbf{x}_1,\mathbf{x}_2\in\mathcal{X} \\ \mathbf{x}_1\neq\mathbf{x}_2}} ||\mathbf{H}_{\mathbb{L}}\left(\mathbf{x}_1 - \mathbf{x}_2\right)||^2 \right\}, \tag{14}$$

where $\mathbf{H}_{\mathbb{L}}$ is the channel matrix of size $n_r \times n_{tu}|\mathbb{S}_{\text{sub}}|$ corresponding to the set $\mathbb{L}$, given by $\mathbf{H}_{\mathbb{L}} = \left[\mathbf{H}^1_{\mathbb{L}}\ \mathbf{H}^2_{\mathbb{L}}\ \cdots\ \mathbf{H}^{n_{tu}}_{\mathbb{L}}\right]$, $\mathbf{H}^j_{\mathbb{L}} = [\mathbf{h}^j_{l_{j1}}\ \mathbf{h}^j_{l_{j2}}\ \cdots\ \mathbf{h}^j_{l_{j|\mathbb{S}_{\text{sub}}|}}]$, l_{j_k} is the kth element in the set $\mathbb{L}^j$, and $\mathcal{X}$ represents the set of all possible transmit vectors. The received signal vector considering this MAP selection is given by

$$\mathbf{y} \quad = \quad \mathbf{H}_{\mathbb{L}_{\text{ED}}}\mathbf{x} + \mathbf{n}. \tag{15}$$

At the receiver, ML detection is performed using the knowledge of the channel matrix $\mathbf{H}_{\mathbb{L}_{\text{ED}}}$. The order of complexity for computing (14) is $\mathcal{O}\left(|\mathcal{L}||\mathcal{X}|^2\right)$, where $|\mathcal{L}| = \binom{|\mathbb{S}_{\text{all}}|}{|\mathbb{S}_{\text{sub}}|}^{n_{tu}}$ and $|\mathcal{X}| = (|\mathbb{S}_{\text{sub}}|M)^{n_{tu}}$.

1) Diversity analysis: In this subsection, we present an analysis of the diversity order achieved by the ED-based MAP selection scheme. We can write $\mathbf{H}_{\mathbb{L}}$ as $\mathbf{H}_{\mathbb{L}} = \mathbf{H}\mathbf{A}_{\mathbb{L}}$, where $\mathbf{H}$ is the channel matrix of size $n_r \times n_{tu}|\mathbb{S}_{\text{all}}|$, given by $\mathbf{H} = \left[\mathbf{H}^1\ \mathbf{H}^2\ \cdots\ \mathbf{H}^{n_{tu}}\right]$, $\mathbf{H}^j = [\mathbf{h}^j_1\ \mathbf{h}^j_2\ \cdots\ \mathbf{h}^j_{|\mathbb{S}_{\text{all}}|}]$, $\mathbf{A}_{\mathbb{L}}$ is the MAP selection matrix of size $n_{tu}|\mathbb{S}_{\text{all}}| \times n_{tu}|\mathbb{S}_{\text{sub}}|$ corresponding to the set $\mathbb{L}$, given by $\mathbf{A}_{\mathbb{L}} = \text{diag}\{\mathbf{A}_{\mathbb{L}^1}, \mathbf{A}_{\mathbb{L}^1}, \cdots, \mathbf{A}_{\mathbb{L}^{n_{tu}}}\}$, and $\mathbf{A}_{\mathbb{L}^j} = [\mathbf{e}_{l_{j1}}\mathbf{e}_{l_{j2}} \cdots \mathbf{e}_{l_{j|\mathbb{S}_{\text{sub}}|}}]$. Note that for every j, $\mathbf{A}_{\mathbb{L}^j}$ can have at most one non-zero element in each row and each column. Now, (14) can be written as

$$\begin{aligned}\mathbb{L}_{\text{ED}} &= \underset{\mathbb{L}\in\mathcal{L}}{\text{argmax}}\left\{\min_{\substack{\mathbf{x}_1,\mathbf{x}_2\in\mathcal{X}\\ \mathbf{x}_1\neq\mathbf{x}_2}} ||\mathbf{H}\mathbf{A}_{\mathbb{L}}\left(\mathbf{x}_1-\mathbf{x}_2\right)||^2\right\}\\ &= \underset{\mathbb{L}\in\mathcal{L}}{\text{argmax}}\left\{\min_{\substack{\mathbf{z}_1,\mathbf{z}_2\in\mathcal{X}_{\mathbb{L}}\\ \mathbf{z}_1\neq\mathbf{z}_2}} ||\mathbf{H}\left(\mathbf{z}_1-\mathbf{z}_2\right)||^2\right\}, \qquad (16)\end{aligned}$$

where $\mathcal{X}_{\mathbb{L}}$ is the set corresponding to $\mathbb{L}$ defined as $\mathcal{X}_{\mathbb{L}} = \{\mathbf{z} : \mathbf{z} = \mathbf{A}_{\mathbb{L}}\mathbf{x}, \mathbf{x}\in\mathcal{X}\}$. Let $\triangle\mathcal{X}_{\mathbb{L}}$ be the set of difference vectors corresponding to the set $\mathcal{X}_{\mathbb{L}}$, i.e., $\triangle\mathcal{X}_{\mathbb{L}} = \{\mathbf{z}_1-\mathbf{z}_2 : \mathbf{z}_1,\mathbf{z}_2 \in \mathcal{X}_{\mathbb{L}}, \mathbf{z}_1 \neq \mathbf{z}_2\}$. Let $\triangle\mathcal{D}$ be the set of matrices defined as

$$\triangle\mathcal{D} = \left\{\mathbf{D} = [\mathbf{d}_1\,\mathbf{d}_2\,\cdots\,\mathbf{d}_{|\mathcal{L}|}] : \mathbf{d}_k \in \triangle\mathcal{X}_{\mathbb{L}_k}, k = 1,\cdots,|\mathcal{L}|\right\},$$

where $\mathbb{L}_k$ is the kth element in the set $\mathcal{L}$. The size of each matrix in $\triangle\mathcal{D}$ is $n_{tu}|\mathbb{S}_{\text{all}}|\times|\mathcal{L}|$. The following proposition gives the diversity order achieved by the ED-based MAP selection scheme in MIMO-MBM.

Proposition 1. *The diversity order achieved by the ED-based MAP selection scheme in MIMO-MBM is given by* $d = n_r\left(|\mathbb{S}_{\text{all}}| - |\mathbb{S}_{\text{sub}}| + 1\right)$.

Proof: The proof is given in the Appendix.

It can be shown that the diversity order achieved by ED-based MAP selection in GSM-MIMO is also given by d.

C. Results and discussion

In Fig. 6, we present a comparison between the BER performance achieved by MIMO-MBM schemes without and with MAP selection. Three schemes, all with $n_{tu} = n_{rf} = 2$, BPSK, 4 bpcu, and $n_r = 2$, are considered. The first scheme is a scheme with no MAP selection, i.e., $M_{rf} = m_{rf} = 1$. The second scheme is a scheme with MI-based MAP selection where $M_{rf} = 2$ and $m_{rf} = 1$. The third scheme is same as the second scheme, except that MAP selection is done based on ED. In all the three schemes, two bits through BPSK symbols (one bit on each MBM-TU) and two bits through RF mirror indexing (one bit on each MBM-TU) result in 4 bpcu. As expected, we observe that the MAP selection schemes achieve better performance compared to the scheme without MAP selection. This is because of the better minimum distance between constellation points achieved by the selection schemes. We also see that ED-based selection achieves significantly better performance compared to MI-based selection. In fact, ED-based selection achieves a higher diversity order compared to MI-based selection. Again, the reason for this is that, because it maximizes the minimum Euclidean distance, the constellation points chosen by ED-based selection have better minimum distance between them compared those chosen by MI-based selection. This can be observed in Fig. 7, which shows the constellation diagrams for the selection schemes with $n_{tu} = n_{rf} = n_r = 1$, $M_{rf} = 5, m_{rf} = 3$, and BPSK. The minimum distance between the constellation points, d_{min}, are 0.0118, 0.3690, and 0.5263 for the schemes without selection, MI-based selection, and ED-based selection, respectively.

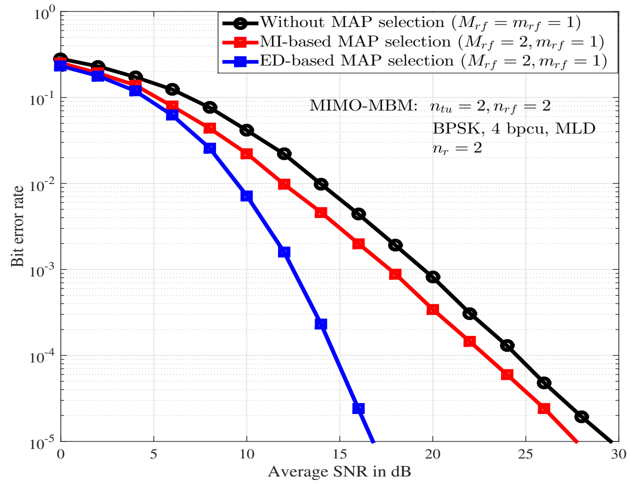

Fig. 6. BER performance comparison between MIMO-MBM schemes without and with MAP selection, $n_{tu} = n_{rf} = 2$, BPSK, 4 bpcu, and $n_r = 2$: *i*) no MAP selection with $M_{rf} = m_{rf} = 1$, *ii*) MI-based MAP selection with $M_{rf} = 2$, $m_{rf} = 1$, and *iii*) ED-based MAP selection with $M_{rf} = 2$, $m_{rf} = 1$.

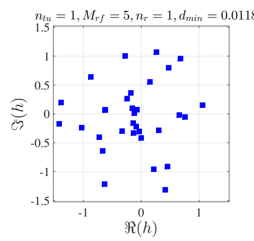

(a) All constellation points

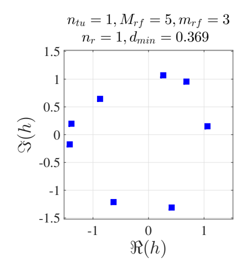

(b) MI-based selection

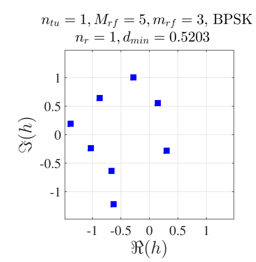

(c) ED-based selection

Fig. 7. Constellation diagrams without and with MAP selection. (a) Set of all constellation points. (b) Constellation points selected by MI-based selection. (c) Constellation points selected by ED-based selection.

Figure 8 presents a validation of the diversity order of ED-based selection predicted by Proposition 1. The slopes of the simulated BER plots in the high SNR regime show that the achieved diversity orders are 3 and 6 for the schemes with $M_{rf} = 2$, $m_{rf} = 1$, and $n_r = 1$ and 2, respectively, which are the same as the ones (i.e., $n_r\left(2^{M_{rf}} - 2^{m_{rf}} + 1\right)$) proved analytically by Proposition 1.

IV. Phase Compensation and Constellation Rotation

In this section, we study the performance of another feedback based transmission scheme called the *phase compensa-*

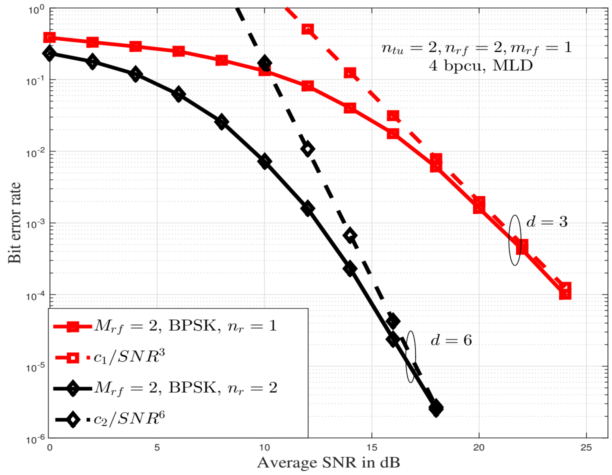

Fig. 8. Diversity orders achieved by ED-based MAP selection in MIMO-MBM for various system parameters.

tion and constellation rotation (PC-CR) scheme. A PC-CR scheme in the context of generalized SSK has been studied in [21]. This scheme exploits the knowledge of the random channel phases (not the amplitudes) at the transmitter to enhance performance. The idea is to co-phase the channels of the active transmit antennas for any spatial-constellation point. That is, the channel phases are compensated at the transmitter, which can be viewed as equal-gain combining (EGC) at the transmitter using knowledge of channel phases at the transmitter. The co-phased spatial-constellation points are further phase-rotated by a deterministic angle which is chosen from $[0, 2\pi)$, so that the minimum Euclidean distance of the constellation points at the receiver is maximized. Here, we study the performance of the PC-CR scheme applied to MIMO-MBM. Consider n_{tu} MBM-TUs at the transmitter, where each MBM-TU uses m_{rf} mirrors. Assume that each MBM-TU transmits a tone.

A. Case of $n_r = 1$

Consider the case when $n_r = 1$. The number of MAPs is $N_m = 2^{m_{rf}}$. For every coherence interval, the receiver estimates all the MBM constellation points, i.e., estimates $h^j_{1,k}$ for every $k \in \{1, 2, \cdots, N_m\}$, $j \in \{1, 2, \cdots, n_{tu}\}$. Let $|h^j_{1,k}|$ and $\phi^j_{1,k}$ denote the magnitude and phase of $h^j_{1,k}$. The receiver feeds back all the phases, i.e., $\phi^j_{1,k}$ for every $k \in \{1, 2, \cdots, N_m\}$, $j \in \{1, 2, \cdots, n_{tu}\}$, to the transmitter. Assume that the feedback is perfect. Using this feedback, the transmitter co-phases (i.e., phase compensates) the channel corresponding to the active MAP in each MBM-TU. Specifically, let $\mathbf{u}$ denote the phase-compensated transmit vector obtained by multiplying the transmit vector $\mathbf{x}$ by phase compensation matrix, given by $\mathbf{W} = \text{diag}\{[(\boldsymbol{\phi}^1_1)^T \ (\boldsymbol{\phi}^2_1)^T \ \cdots (\boldsymbol{\phi}^{n_{tu}}_1)^T]\}$, where $\boldsymbol{\phi}^j_1 = [e^{-\imath\phi^j_{1,1}} \ e^{-\imath\phi^j_{1,2}} \ \cdots \ e^{-\imath\phi^j_{1,N_m}}]^T$, $j \in \{1, 2, \cdots, n_{tu}\}$, and $\imath = \sqrt{-1}$.

Let $\mathbb{U}_{\text{pc}} \triangleq \{\mathbf{u} : \mathbf{u} = \mathbf{W}\mathbf{x}, \mathbf{x} \in \mathcal{X}\}$, denote the phase-compensated signal set, where $\mathcal{X}$ represents the set of all possible transmit vectors without phase compensation. After phase compensation, the resultant phase-compensated transmit vectors are further rotated to improve performance. Specifically, denoting the kth vector in $\mathbb{U}_{\text{pc}}$ as $\mathbf{u}_k$, each element in $\mathbf{u}_k$ is rotated by the angle ψ_k. The rotation angles $\{\psi_k\}_{k=1}^{|\mathcal{X}|}$ are chosen such that the minimum Euclidean distance of the constellation at the receiver is maximized. The optimum angles are obtained as the solution to the following optimization problem:

$$\{\hat{\psi_k}\} = \underset{\substack{\psi_k \in [0, 2\pi) \\ \forall k}}{\text{argmax}} \left\{ \min_{\substack{\mathbf{u}_{k_1}, \mathbf{u}_{k_2} \in \mathbb{U}_{\text{pc}} \\ k_1 \neq k_2}} \| \tilde{\mathbf{h}}_1^T \big(\mathbf{u}_{k_1} e^{\imath\psi_{k_1}} - \mathbf{u}_{k_2} e^{\imath\psi_{k_1}} \big) \|^2 \right\},$$

where $\tilde{\mathbf{h}}_1 = [h^1_{1,1} \cdots h^1_{1,N_m} h^2_{1,1} \cdots h^2_{1,N_m} \cdots h^{n_{tu}}_{1,1} \cdots h^{n_{tu}}_{1,N_m}]^T$. Taking a geometrical view of the above optimization problem, we can see that its solution is given by $\hat{\psi_k} = (k-1)2\pi/|\mathcal{X}|$.

Let $\mathbb{V}_{\text{pc-cr}}$ denote the resulting signal set after phase compensation and constellation rotation described above. The kth vector in $\mathbb{V}_{\text{pc-cr}}$, denoted by $\mathbf{v}_k$, is then given by $e^{\imath\hat{\psi_k}}\mathbf{u}_k$. The received signal at the receiver can be written as

$$y = \tilde{\mathbf{h}}_1^T \mathbf{v} + n, \tag{17}$$

and the corresponding ML decision rule is given by

$$\hat{\mathbf{v}} = \underset{\mathbf{v} \in \mathbb{V}_{\text{pc-cr}}}{\text{argmin}} \ |y - \tilde{\mathbf{h}}_1^T \mathbf{v}|^2. \tag{18}$$

Now, from $\hat{\mathbf{v}}$, the detected $\mathbf{x}$ vector, denoted by $\hat{\mathbf{x}}$, can be obtained as $\hat{\mathbf{x}} = (\hat{\mathbf{v}}^\dagger)^T \odot \hat{\mathbf{v}}$, where $\odot$ denotes the element-wise multiplication operator. The $\hat{\mathbf{x}}$ vector is demapped to get the corresponding information bits.

Performance: Figure 9 shows the BER performance of MIMO-MBM without and with PC-CR, for $n_{tu} = n_{rf} = 2$, $m_{rf} = 1$, tone, 2 bpcu, $n_r = 1$, and ML detection. It can be seen that the feedback based PC-CR scheme significantly improves the BER performance. This is because of the maximization of the minimum ED at the receiver in the PC-CR scheme.

B. Case of $n_r > 1$

When there are more than one receive antenna, the phase compensation presented in the previous subsection for $n_r = 1$ is not directly applicable, since there are $n_r > 1$ complex-valued channels between each MBM-TU and the receiver. Let $\tilde{\mathbf{h}}_k = [h^1_{k,1} \ \cdots \ h^1_{k,N_m} \ h^2_{k,1} \ \cdots \ h^2_{k,N_m} \cdots \ h^{n_{tu}}_{k,1} \ \cdots \ h^{n_{tu}}_{k,N_m}]^T$ denote the channel coefficient vector of size $N_m n_{tu} \times 1$ of the kth receive antenna, $k = 1, 2, \cdots, n_r$. Here, we present two receiver schemes for phase compensation when $n_r > 1$.

1) Receiver scheme 1: A possible extension of phase compensation for multiple receive antennas ($n_r > 1$) is presented in [22], in which the upper bound on the conditional BEP for the ML decision rule in (18) is evaluated for each receive antenna and the receive antenna with the lowest upper bound is selected. We refer this scheme as receiver scheme 1 (Rx. scheme 1). The upper bound on the conditional BEP (i.e.,

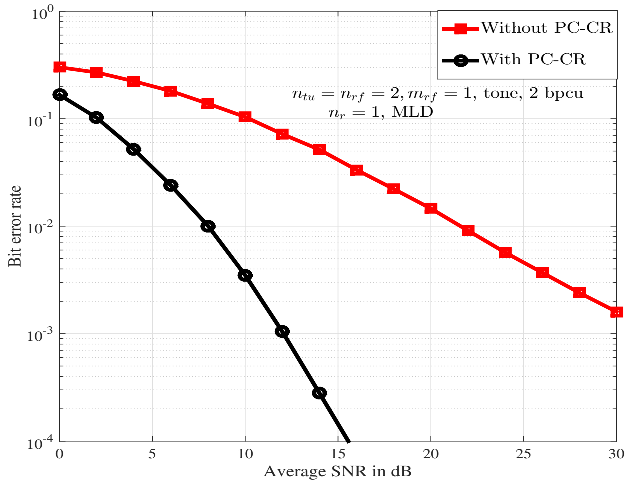

Fig. 9. BER performance of MIMO-MBM without and with PC-CR, for $n_{tu} = n_{rf} = 2$, $m_{rf} = 1$, tone, 2 bpcu, $n_r = 1$, and ML detection.

given $\tilde{\mathbf{h}}_k$) for ML detection in (18) is given by

$$P_{B|\tilde{\mathbf{h}}_k} \leq \frac{1}{2^\eta} \sum_{\mathbf{v}_1} \sum_{\mathbf{v}_2 \neq \mathbf{v}_1} P\left(\mathbf{v}_1 \to \mathbf{v}_2 | \tilde{\mathbf{h}}_k\right) \frac{\delta(\mathbf{v}_1, \mathbf{v}_2)}{\eta}$$
$$= \frac{1}{2^\eta} \sum_{\mathbf{v}_1} \sum_{\mathbf{v}_2 \neq \mathbf{v}_1} Q\left(\sqrt{\frac{|\tilde{\mathbf{h}}_k^T (\mathbf{v}_1 - \mathbf{v}_2)|^2}{2\sigma^2}}\right) \frac{\delta(\mathbf{v}_1, \mathbf{v}_2)}{\eta}. \quad (19)$$

The receiver selects the receive antenna with lowest upper bound, i.e.,

$$\hat{k} = \underset{k \in \{1,2,\cdots,n_r\}}{\text{argmin}} \; P_{B|\tilde{\mathbf{h}}_k}. \quad (20)$$

The receiver feeds back all the phases of $\mathbf{h}_{\hat{k}}$. Let $\mathbb{V}_{\text{pc-cr}}^{\hat{k}}$ denote signal set corresponding to the phase compensation and constellation rotation defined as in Sec. IV-A. Only the selected receive antenna (i.e., $\hat{k}$) will be active and others will be silent. The received signal can then be written as

$$y = \tilde{\mathbf{h}}_{\hat{k}}^T \mathbf{v} + n, \quad (21)$$

and the corresponding ML decision rule is given by

$$\hat{\mathbf{v}} = \underset{\mathbf{v} \in \mathbb{V}_{\text{pc-cr}}^{\hat{k}}}{\text{argmin}} \; |y - \tilde{\mathbf{h}}_{\hat{k}}^T \mathbf{v}|^2. \quad (22)$$

Now, from $\hat{\mathbf{v}}$, the detected $\mathbf{x}$ vector, denoted by $\hat{\mathbf{x}}$, can be obtained as $\hat{\mathbf{x}} = (\hat{\mathbf{v}}^\dagger)^T \odot \hat{\mathbf{v}}$. A drawback in this scheme is that it uses only one antenna to receive signal even though multiple antennas are available at the receiver. To overcome this drawback, we present another possible extension of phase compensation scheme for multiple receive antennas, referred as receiver scheme 2 (Rx. scheme 2) in which signals from all the receive antennas will be used for detection.

2) Receiver scheme 2: The receiver selects the receive antenna for phase compensation as in Sec. IV-B1, and feeds back its corresponding phases to the transmitter. Let $\hat{k}$ denote the selected receive antenna, and let $\mathbb{V}_{\text{pc-cr}}^{\hat{k}}$ denote signal set corresponding to the phase compensation and constellation rotation. The signals from all the receive antennas are used. Then, the received signal vector is given by

$$\mathbf{y} = \mathbf{H}\mathbf{v} + \mathbf{n}, \quad (23)$$

where $\mathbf{H}$ is $n_r \times N_m n_{tu}$ channel matrix given by $\mathbf{H} = [\tilde{\mathbf{h}}_1 \; \tilde{\mathbf{h}}_2 \; \cdots \; \tilde{\mathbf{h}}_{n_r}]^T$. Since phase compensation is carried out based on the phases of $\hat{k}$th receive antenna, the effect of phase compensation needs to be eliminated at other receive antennas. To account for this, we present the modified decision rule as follows:

$$\hat{\mathbf{v}} = \underset{\mathbf{v} \in \mathbb{V}_{\text{pc-cr}}^{\hat{k}}}{\text{argmin}} \; \|\mathbf{y} - \mathbf{H}^{(\mathbf{v})}\mathbf{v}\|^2, \quad (24)$$

where $\mathbf{H}^{(\mathbf{v})} \triangleq [\tilde{\mathbf{h}}_1^{(\mathbf{v})} \cdots \tilde{\mathbf{h}}_{\hat{k}}^{(\mathbf{v})} \cdots \tilde{\mathbf{h}}_{n_r}^{(\mathbf{v})}]^T$, and $\tilde{\mathbf{h}}_i^{(\mathbf{v})}$'s are given by

$$\tilde{\mathbf{h}}_i^{(\mathbf{v})} \triangleq \begin{cases} \tilde{\mathbf{h}}_i & \text{if } i = \hat{k} \\ \tilde{\mathbf{h}}_i \odot (\mathbf{v}^\dagger)^T & \text{if } i \neq \hat{k}. \end{cases} \quad (25)$$

Since $\mathbf{x} = (\hat{\mathbf{v}}^\dagger)^T \odot \hat{\mathbf{v}}$, we have $(\tilde{\mathbf{h}}_i^{(\mathbf{v})})^T \mathbf{v} = \tilde{\mathbf{h}}_i^T \mathbf{x}$ for $i \neq \hat{k}$. Now, (24) becomes

$$\begin{aligned} \hat{\mathbf{v}} &= \underset{\mathbf{v} \in \mathbb{V}_{\text{pc-cr}}^{\hat{k}}}{\text{argmin}} |y_{\hat{k}} - \tilde{\mathbf{h}}_{\hat{k}}^T \mathbf{v}|^2 + \sum_{i \neq \hat{k}} |y_i - \tilde{\mathbf{h}}_i^T ((\hat{\mathbf{v}}^\dagger)^T \odot \hat{\mathbf{v}})|^2 \\ &= \underset{\mathbf{v} \in \mathbb{V}_{\text{pc-cr}}^{\hat{k}}}{\text{argmin}} |y_{\hat{k}} - \tilde{\mathbf{h}}_{\hat{k}}^T \mathbf{v}|^2 + \sum_{i \neq \hat{k}} |y_i - \tilde{\mathbf{h}}_i^T \mathbf{x}|^2. \end{aligned} \quad (26)$$

From (26), we can see that this decision rule gives the advantage of both phase compensation (by $\hat{k}$th receive antenna) and SNR gain by using other $n_r - 1$ receive antennas.

Performance: Figure 9 shows the BER performance of MIMO-MBM without PC-CR, with PC-CR using Rx. scheme 1 and Rx. scheme 2, for $n_{tu} = n_{rf} = 2$, $m_{rf} = 1$, tone, 2 bpcu, $n_r = 3$, and ML detection. It can be seen that the Rx. scheme 2 performs better than Rx. scheme 2 by about 1.5 dB at 10^{-5} BER. This is because Rx. scheme 2 uses signals from all the receive antennas for detection, whereas Rx. scheme 1 uses the signal only from the selected receive antenna.

V. Conclusion

We investigated the performance of some interesting physical layer techniques when applied to media-based modulation (MBM), which is a recently proposed modulation scheme that uses RF mirrors to perturb the propagation environment to create independent channel fade realizations which themselves are used as the constellation points. The considered physical layer techniques included generalized spatial modulation (GSM), mirror activation pattern (MAP) selection (analogous to antenna selection in MIMO systems), and phase compensation and constellation rotation. It was shown that, for the same spectral efficiency, GSM-MBM can achieve better performance compared to MIMO-MBM. The Euclidean distance based MAP selection scheme was found to perform better than the mutual information based MAP selection scheme by several dBs. The diversity order achieved by the Euclidean distance based MAP selection scheme was shown to be $n_r(2^{M_{rf}} - 2^{m_{rf}} + 1)$, which was also validated through

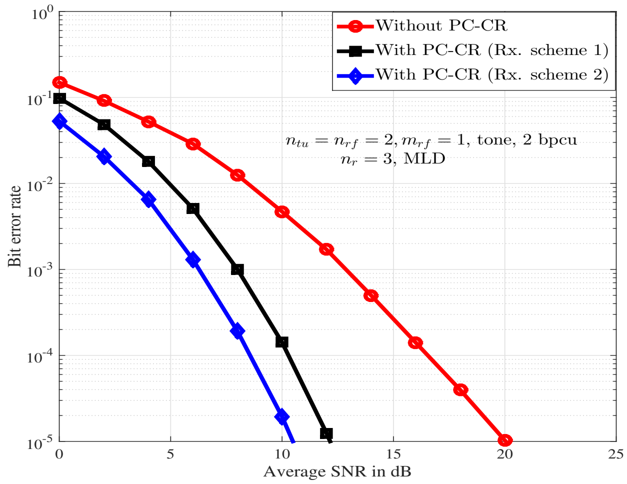

Fig. 10. BER performance of MIMO-MBM without PC-CR, with PC-CR using Rx. scheme 1 and Rx. scheme 2, for $n_{tu} = n_{rf} = 2$, $m_{rf} = 1$, tone, 2 bpcu, $n_r = 3$, and ML detection.

simulations. Feedback based phase compensation and MBM constellation rotation was found to increase the Euclidean distance between the constellation points, thereby improving the bit error performance significantly.

Appendix

Proof of Proposition 1

Proof: Let $p = \min\{rank\,(\mathbf{D}) : \mathbf{D} \in \triangle\mathcal{D}\}$. Using Proposition 1 in [23], the diversity order achieved by ED based MAP selection is given by $n_r p$. Any matrix $\mathbf{D} \in \triangle\mathcal{D}$ can be viewed in the form $\mathbf{D} = [\mathbf{D}_1^T \ \mathbf{D}_2^T \ \cdots \ \mathbf{D}_{n_{tu}}^T]^T$, where $\mathbf{D}_j$ is a sub-matrix of size $|\mathbb{S}_{\text{all}}| \times |\mathcal{L}|$. Consider a matrix $\mathbf{D} \in \triangle\mathcal{D}$ which is constrained such that only one sub-matrix (say, $\mathbf{D}_k$) is a non-zero sub-matrix and all other sub-matrices ($\mathbf{D}_j$'s, $j \neq k$) are zero sub-matrices. That is, the constrained matrix is of the form $\mathbf{D} = [\mathbf{0}^T \ \mathbf{0}^T \ \cdots \ \mathbf{D}_k^T \ \cdots \ \mathbf{0}^T \ \mathbf{0}^T]^T$, $k \in \{1, 2, \cdots, n_{tu}\}$. Therefore, $rank(\mathbf{D}) = rank(\mathbf{D}_k)$. Any matrix in $\triangle\mathcal{D}$ which does not have the above constraint can be obtained by replacing one or more zero sub-matrices by non-zero sub-matrices. Since a rank of a matrix will not reduce if some of its zero rows/columns are replaced by non-zero rows/columns, the minimum rank is obtained by matrices with the above constraint.

Let $\triangle\mathbb{A}$ denote the set of non-zero difference QAM/PSK constellation points, given by $\{s_1 - s_2 : s_1, s_2 \in \mathbb{A}, s_1 \neq s_2\}$. Note that every column of $\mathbf{D}_k$ is either from the set $\mathcal{E}_l \triangleq \{c\mathbf{e}_l : c \in \triangle\mathbb{A}\}$ for $1 \leq l \leq |\mathbb{S}_{\text{all}}|$ or from the set $\mathcal{E}_{l,q} \triangleq \{s_1\mathbf{e}_l + s_2\mathbf{e}_q : s_1, s_2 \in \mathbb{A}\}$ for $1 \leq l \neq q \leq |\mathbb{S}_{\text{all}}|$. Now, using Proposition 2 of [23], the minimum rank of $\mathbf{D}_k$ is $|\mathbb{S}_{\text{all}}| - |\mathbb{S}_{\text{sub}}| + 1$. Hence, $p = \min\{rank\,(\mathbf{D}) : \mathbf{D} \in \triangle\mathcal{D}\} = |\mathbb{S}_{\text{all}}| - |\mathbb{S}_{\text{sub}}| + 1$. Therefore, the diversity order achieved by ED-based MAP selection is $n_r\,(|\mathbb{S}_{\text{all}}| - |\mathbb{S}_{\text{sub}}| + 1)$.

Acknowledgment

This work was supported in part by the J. C. Bose National Fellowship, Department of Science and Technology, Government of India.

References

[1] Y. A. Chau and S.-H. Yu, "Space modulation on wireless fading channels," in *Proc. IEEE 54th VTC'2001 (Fall)*, vol. 3, Oct. 2001, pp. 1668-1671.

[2] J. Jeganathan, A. Ghrayeb, L. Szczecinski, and A. Ceron, "Space shift keying modulation for MIMO channels," *IEEE Trans. Wireless Commun.,* vol. 8, no. 7, pp. 3692-3703, Jul. 2009.

[3] A. K. Khandani, "Media-based modulation: A new approach to wireless transmission," in *Proc. IEEE ISIT'2013*, Jul. 2013, pp. 3050-3054.

[4] A. K. Khandani, "Media-based modulation: Converting static Rayleigh fading to AWGN," in *Proc. IEEE ISIT'2014*, Jun-Jul. 2014, pp. 1549-1553.

[5] A. K. Khandani, "Media-based modulation: A new approach to wireless transmission," Tech. Rep., University of Waterloo, Canada. Online: http://www.cst.uwaterloo.ca/reports/media-report.pdf

[6] E. Seifi, M. Atamanesh, and A. K. Khandani, "Media-based modulation: A new frontier in wireless communications," online: arXiv:1507.07516v3 [cs.IT] 7 Oct 2015.

[7] R. Mesleh, H. Haas, S. Sinanovic, C. W. Ahn, and S. Yun, "Spatial modulation," *IEEE Trans. Veh. Tech.*, vol. 57, no. 4, pp. 2228-2241, Jul. 2008.

[8] M. Di Renzo, H. Haas, A. Ghrayeb, S. Sugiura, and L. Hanzo, "Spatial modulation for generalized MIMO: Challenges, opportunities and implementation," *Proceedings of the IEEE*, vol. 102, no. 1, pp. 56-103, Jan. 2014.

[9] A. Chockalingam and B. S. Rajan, *Large MIMO Systems*, Cambridge Univ. Press, Feb. 2014.

[10] J. Wang, S. Jia, and J. Song, "Generalised spatial modulation system with multiple active transmit antennas and low complexity detection scheme," *IEEE Trans. Wireless Commun.*, vol. 11, no. 4, pp. 1605-1615, Apr. 2012.

[11] T. Datta and A. Chockalingam, "On generalized spatial modulation," in *Proc. IEEE WCNC'2013*, Apr. 2013, pp. 2716-2721.

[12] T. Lakshmi Narasimhan and A. Chockalingam, "On the capacity and performance of generalized spatial modulation," *IEEE Commun. Lett.*, DOI: 10.1109/LCOMM.2015.2497255.

[13] R. Abu-alhiga and H. Haas, "Subcarrier index modulation OFDM," in *Proc. IEEE PIMRC'2009*, Sep. 2009, pp. 177-181.

[14] D. Tsonev, S. Sinanovic, and H. Haas, "Enhanced subcarrier index modulation (SIM) OFDM," in *Proc. IEEE GLOBECOM'2011*, Dec. 2011. pp. 728-732.

[15] E. Basar, U. Aygolu, E. Panayirci, and H. V. Poor, "Orthogonal frequency division multiplexing with indexing," in *Proc. IEEE GLOBECOM'2012*, Dec. 2012, pp. 4741-4746.

[16] Y. Xiao, S. Wang, L. Dan, X. Lei, P. Yang, and W. Xiang, "OFDM with interleaved subcarrier-index modulation," *IEEE Commun. Lett.*, vol. 8, no. 8, pp. 1447-1450, Aug. 2014.

[17] T. Datta, H. Eshwaraiah, and A. Chockalingam, "Generalized space and frequency index modulation," *IEEE Trans. Veh. Tech.*, DOI 10.1109/TVT.2015.2451095.

[18] T. Lakshmi Narasimhan, Y. Naresh, T. Datta, and A. Chockalingam, "Pseudo-random phase precoded spatial modulation and precoder index modulation," in *Proc. IEEE GLOBECOM'2014*, Nov. 2014, pp. 3868-3873.

[19] M. S. Alouini and A. Goldsmith, "A unified approach for calculating error rates of linearly modulated signals over generalized fading channels," *IEEE Trans. Commun.*, vol. 47, no. 9, pp. 1324-1334, Sep. 1999.

[20] R. Rajashekar, K. V. S. Hari, and L. Hanzo, "Antenna selection in spatial modulation systems," *IEEE Commun. Lett.*, vol. 17, no. 3, pp. 521-524, Mar. 2013.

[21] K. Ntontin, M. Di Renzo, , A. Perez-Neira, and C. Verikoukis, "Adaptive generalized space shift keying," *EURASIP J. Wireless Commun. and Netw.*, 2013, 2013:43.

[22] M. S. Veedu, C. R. Murthy, and L. Hanzo, "Single-RF spatial modulation relying on finite-rate phase-only feedback: Design and analysis," *IEEE Trans. Veh. Tech.*, DOI 10.1109/TVT.2015.2424960.

[23] R. Rajashekar, K. V. S. Hari, and L. Hanzo, "Quantifying the transmit diversity order of Euclidean distance based antenna selection in spatial modulation," *IEEE Signal. Process. Lett.*, vol. 22, no. 9, pp. 1434-1437, Sep. 2015.